Science Advances

AAAS

advances.sciencemag.org/cgi/content/full/2/4/e1501693/DC1

Supplementary Materials for

Climate-driven polar motion: 2003–2015

Surendra Adhikari and Erik R. Ivins

Published 8 April 2016, *Sci. Adv.* **2**, e1501693 (2016)
DOI: 10.1126/sciadv.1501693

The PDF file includes:

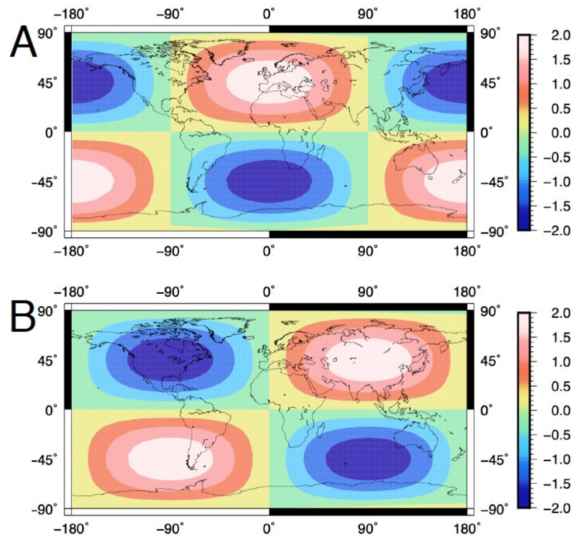

fig. S1. SHs of degree 2 order 1. (**A**) Cosine term that corresponds with $\chi_1(t)$. (**B**) Sine term that corresponds with $\chi_2(t)$. Color scales are associated with 4π-normalization (*18, 34*).

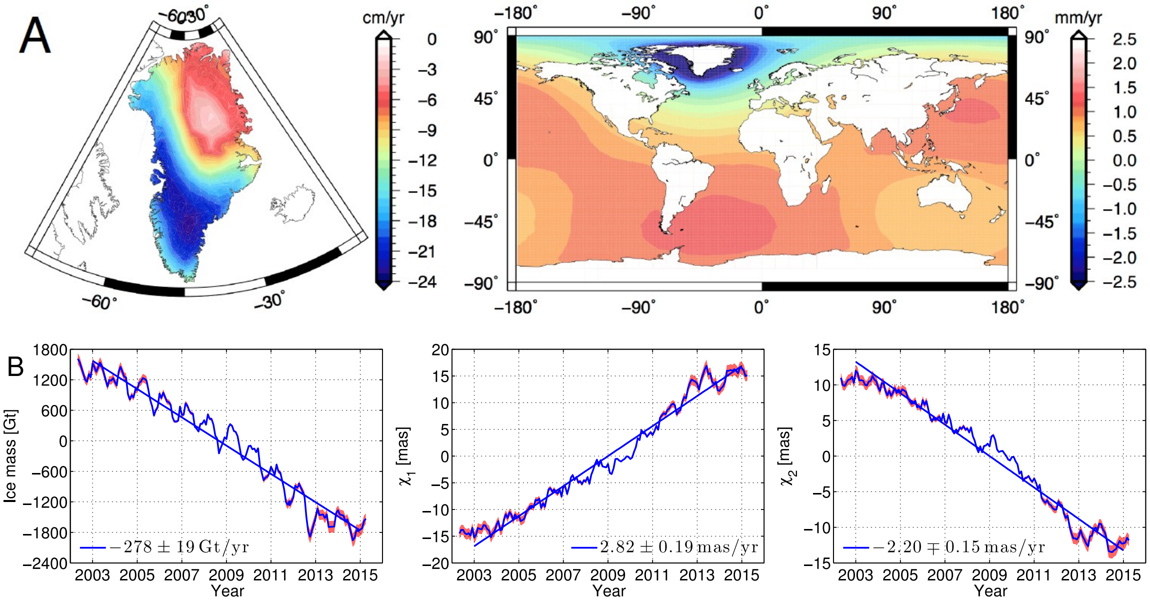

fig. S2. GIS and polar motion excitations. (**A**) Linear trend in $L(\theta, \lambda, t)$ during the study period. Spatial distribution of rate of change in ice thickness (left) and associated sea-level fingerprint (right) are shown. (**B**) Mass evolution of GIS (left) and the corresponding polar motion excitations. Solutions are plotted with respect to the corresponding 2003-2015 mean values.

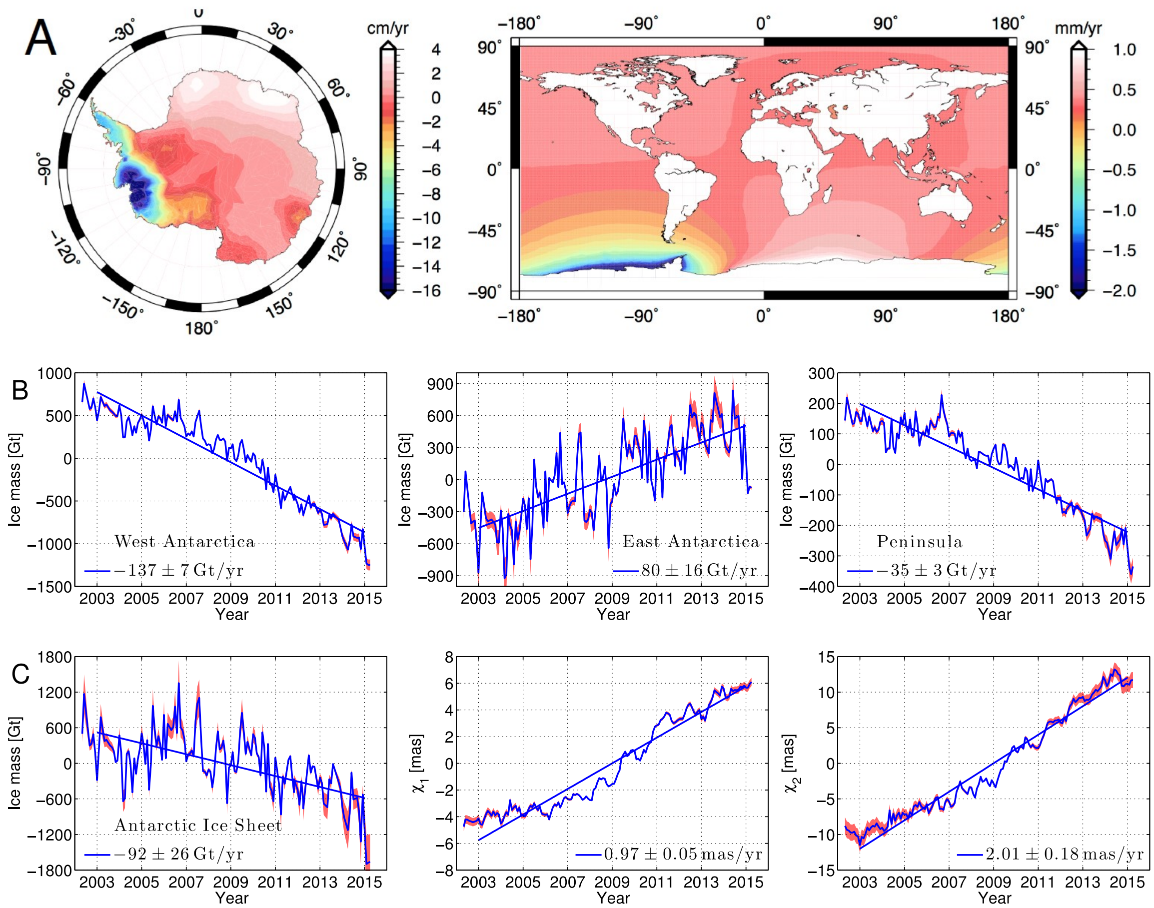

fig. S3. AIS and polar motion excitations. (**A**) Linear trend in $L(\theta, \lambda, t)$ during the study period. Spatial distribution of rate of change in ice thickness (left) and associated sea-level fingerprint (right) are shown. (**B**) Mass evolution of West AIS (left), East AIS (middle), and Antarctic Peninsula (right). (**C**) Mass evolution of the entire AIS (left) and the corresponding polar motion excitations. Solutions are plotted with respect to the corresponding 2003-2015 mean values.

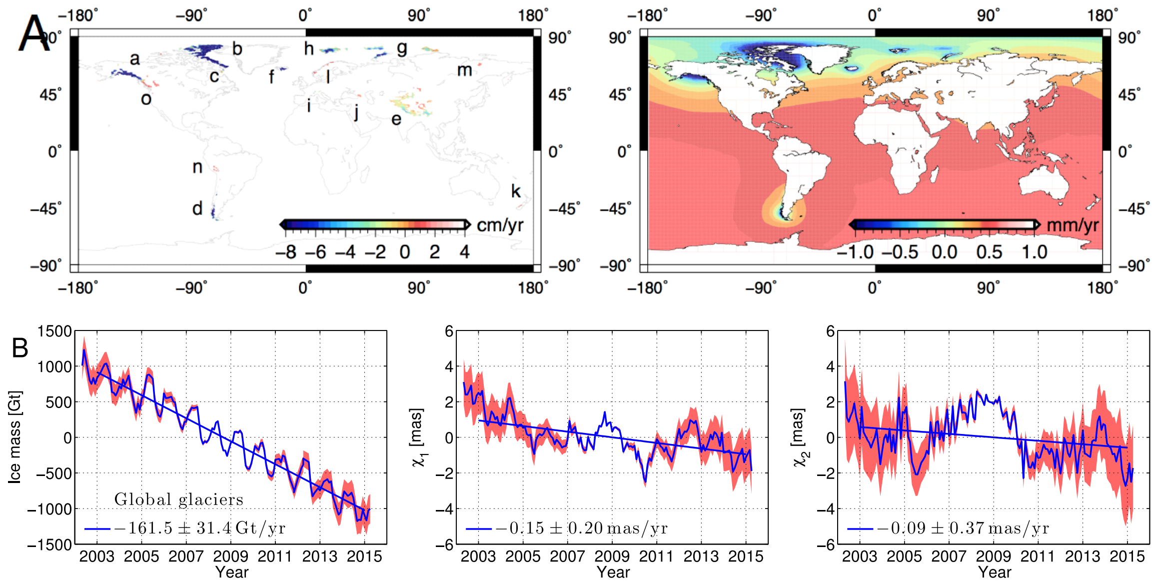

fig. S4. Global GICs and polar motion excitations. (**A**) Linear trend in $L(\theta, \lambda, t)$ during the study period. Spatial distribution of rate of change in ice thickness (left) and associated sea-level fingerprint (right) are shown. Fifteen glaciated regions are annotated (a-o); corresponding mass evolution are summarized in fig. S5. (**B**) Mass evolution of global GICs (left) and the corresponding polar motion excitations. Solutions are plotted with respect to the corresponding 2003-2015 mean values.

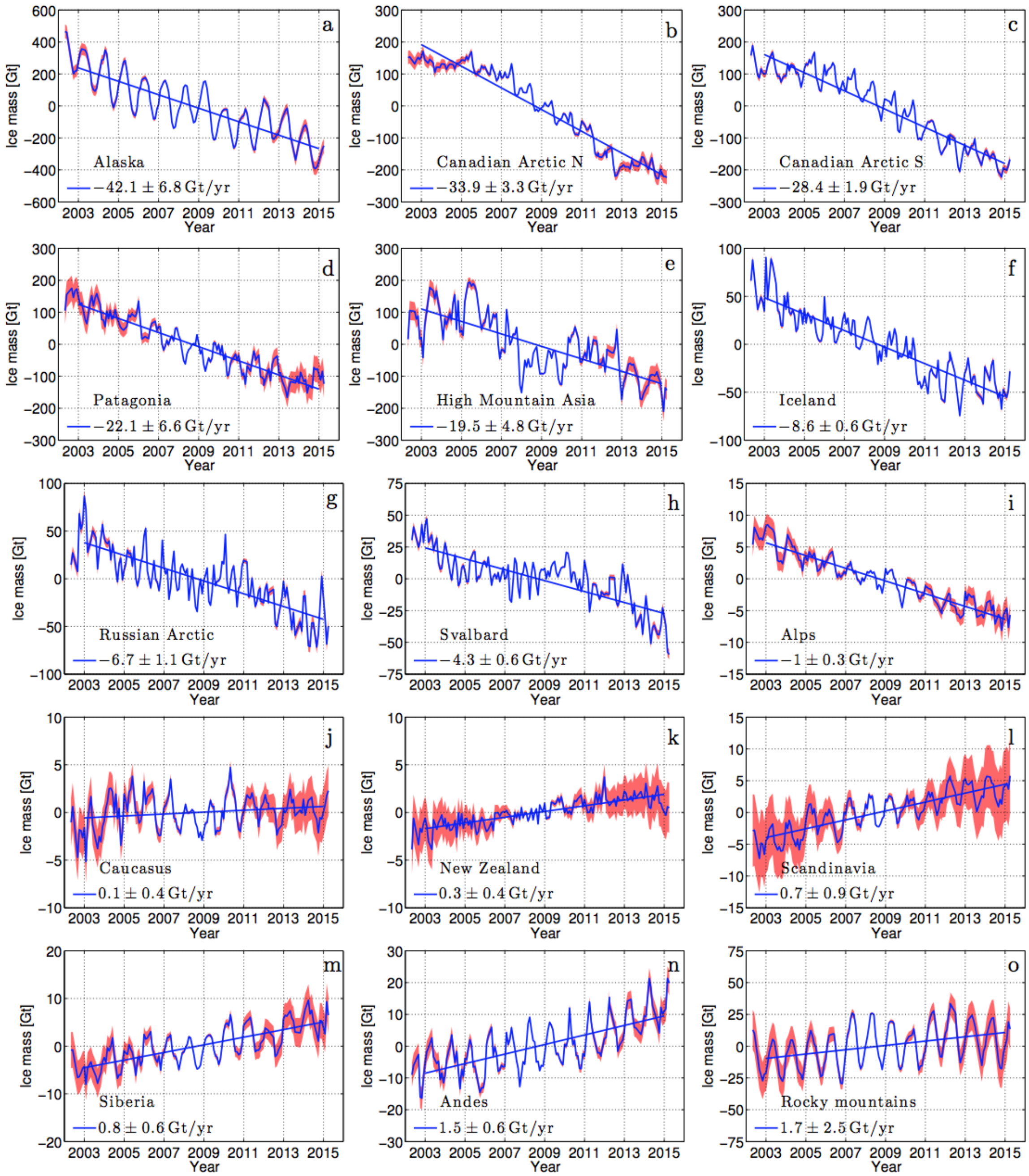

fig. S5. Mass evolution of regional GICs. See fig. S4 for coordinates of individual glaciated regions. These regions have decreasing trends in mass loss. Solutions are plotted with respect to the corresponding 2003-2015 mean values.

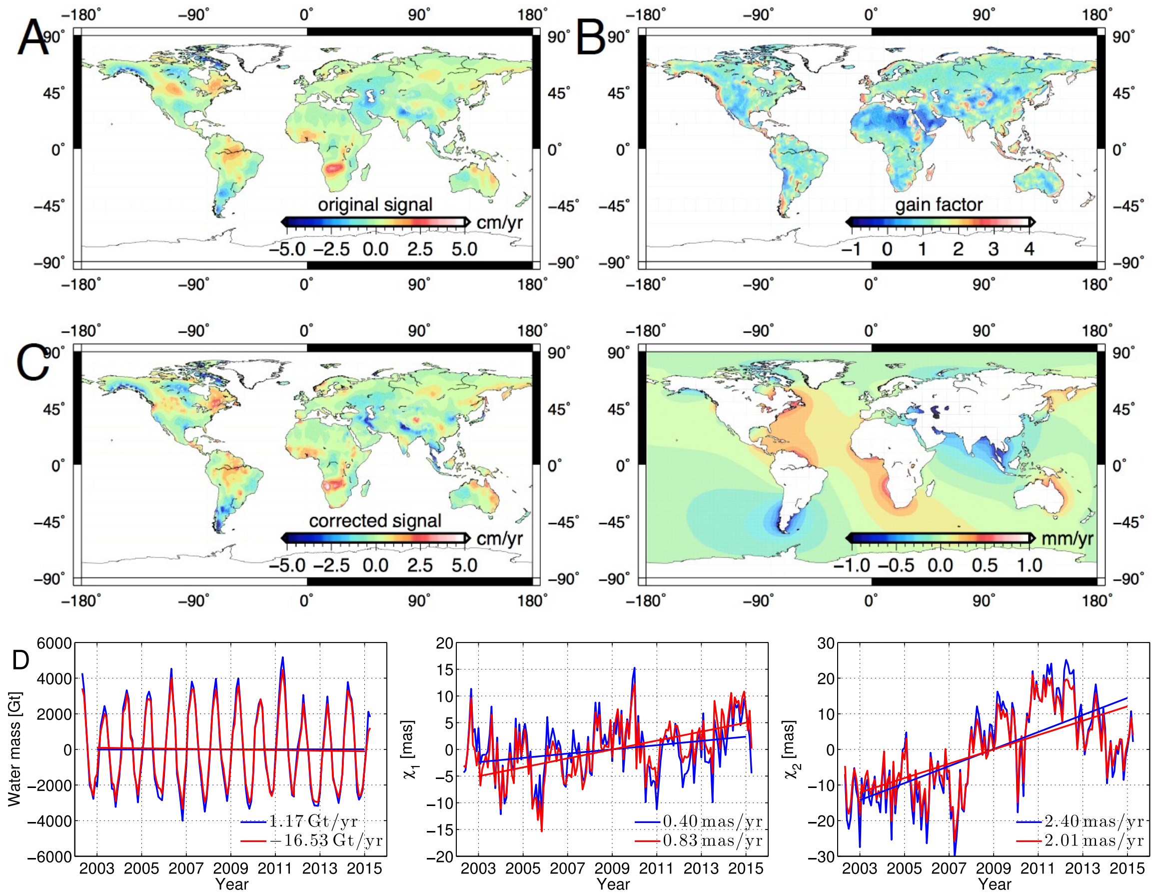

fig. S6. TWS and polar motion excitations. (**A**) TWS signal (in WEH per year) derived from the standard GRACE solutions. (**B**) Signal gain factors (*17*) to restore the attenuated signals. (**C**) Corrected TWS signal (left) and associated sea-level fingerprint (right). (**D**) Mass evolution of TWS (left) and the corresponding polar motion excitations. Red and blue lines represent original and corrected (with gain factors applied) signals, respectively. Solutions are plotted with respect to the corresponding 2003-2015 mean values.

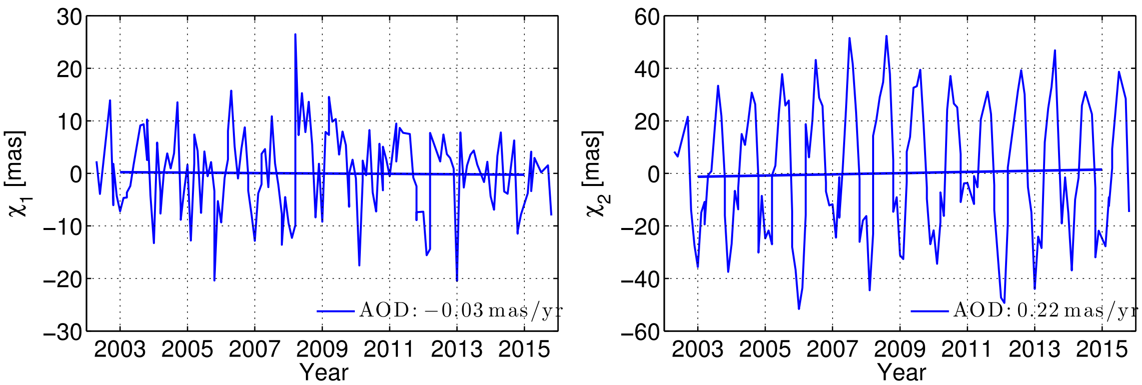

fig. S7. Polar motion excitations due to nontidal AOM variability. Solutions are based on complementary GRACE Release-05 Level-2 GAC data products. Seasonal signals are much larger, as expected, than those associated with cryosphere.

	2003-2015	2005-2011	2012-2015
GIS	(2.82±0.19, −2.20∓0.15)	(2.76, −2.18)	(2.07, −1.60)
AIS	(0.97±0.05, 2.01±0.18)	(1.14, 1.97)	(0.84, 2.13)
GICs	(−0.15±0.20, −0.09±0.37)	(−0.15, −0.09)	(−0.67, −0.08)
TWS	(0.40±0.43, 2.40±0.39)	(0.52, 4.97)	(4.01, −7.98)
AOM	(−0.03, 0.22)	(−0.03, 0.22)	(−0.03, 0.22)
Reconstructed	(4.01±0.87, 2.34±1.09)	(4.24, 4.89)	(6.22, −7.31)
Observed	(4.60±0.20, 3.06±0.74)	(6.38, 6.22)	(3.45, −3.94)

table S1. Polar motion excitation rates for different time periods. Solutions are tabulated as (χ_1, χ_2). The 20th century linear trends, $\dot{\chi}_1(t) = 0.79$ mas/yr and $\dot{\chi}_2(t) = -2.95$ mas/yr, are removed from the observed data (see Materials and Methods). Uncertainty ranges for 2005-2011 and 2012-2015 are similar to the corresponding values listed for 2003-2015, and hence not explicitly noted.